Endobronchial Ultrasound Doppler Image Features Correlate with mRNA Expression of HIF1-α and VEGF-C in Patients with Non–Small-Cell Lung Cancer

Takahiro Nakajima, MD, PhD,†‡ Takashi Anayama, MD, PhD,* Terumoto Koike, MD, PhD,* Masato Shingyoji, MD, PhD,† Lianne Castle, MD, PhD,* Hideki Kimura, MD, PhD,† Ichiro Yoshino, MD, PhD,‡ and Kazuhiro Yasufuku MD, PhD**

Introduction: We attempted to assess the correlation between the Doppler mode image patterns during endobronchial ultrasound-guided (EBUS) transbronchial needle aspiration and the expression of angiogenesis-related molecules within lymph nodes in patients with non–small-cell lung cancer.

Methods: Thirty-eight archived EBUS- transbronchial needle aspiration samples of lymph nodes (27 metastatic and 11 nonmetastatic) in patients with non–small-cell lung cancer with Doppler mode ultrasound image were analyzed. The Doppler mode image of the vasculature of the targeted lymph node was categorized into the following groups: normal blood flow, low blood flow (LBF), and high blood flow (HBF). Vascular index ratio (vascular area/lymph node area) of each metastatic lymph node was calculated. Total RNA and protein was extracted and analyzed for expression of *HIF-1α*, *VEGF-A*, and *VEGF-C* by quantitative RT-PCR and enzyme-linked immunosorbent assay.

Results: Within the 27 metastatic lymph nodes, eight were categorized into the LBF group and 19 into the HBF group. Vascular index ratio was significantly higher in HBF than LBF ($p = 0.0003$). mRNA expression of *HIF-1α* and *VEGF-A* was significantly higher in metastatic lymph nodes than in benign lymph nodes ($p < 0.0001$). Compared with LBF and HBF, *HIF-1α* mRNA expression was significantly higher in LBF ($p = 0.01$) and *VEGF-C* mRNA expression was significantly higher in HBF ($p = 0.0315$). There was no significant difference in protein expression by enzyme-linked immunosorbent assay analysis.

Conclusions: The vascularity of metastatic lymph nodes observed by EBUS correlates with the mRNA expression of *HIF-1α* and *VEGF-C* (not *VEGF-A*). This correlation is a clinical utility that needs to be evaluated further.

*Division of Thoracic Surgery, Toronto General Hospital, University Health Network, Toronto, Canada; †Division of Thoracic Diseases, Chiba Cancer Center, Chiba, Japan; and ‡Department of General Thoracic Surgery, Graduate School of Medicine, Chiba University, Chiba, Japan.

Disclosure: TN has been supported by a Research Fellowship from "Kanae Foundation for The Promotion of Medical Science" for the study in Toronto and received the Wanda Plachta Fellowship in Lung Cancer Research. KY has received grants from Olympus Medical Systems for continuing medical education and research. The other authors declare no conflicts of interest.

Address for correspondence: Takahiro Nakajima, MD, PhD, Graduate School of Medicine, 1-7-1, Inohana, Chuo-ku, Chiba, JAPAN. E-mail: nakajii@fc.med.miyazaki-u.ac.jp

ISSN: 1556-0864/12/0711-1661

Key Words: Doppler mode imaging, Endobronchial ultrasound, Non–small-cell lung cancer, Lymph node metastasis, Tumor angiogenesis and lymphangiogenesis.

(*J Thorac Oncol.* 2012;7: 1661–1667)

Endobronchial ultrasound-guided transbronchial needle aspiration (EBUS-TBNA) is a minimally invasive modality with a high diagnostic yield for mediastinal staging of non–small cell lung cancer (NSCLC).[1–3] EBUS-TBNA is a biopsy procedure, but the EBUS ultrasound image itself may also be helpful for the prediction of lymph node metastasis.[4] Metastatic tumor affects the lymph node structure and vascularity. We have previously reported a standard EBUS image classification system for lymph nodes.[5] In addition, we have recently reported a standard EBUS Doppler mode vascular image classification system for lymph nodes.[6] We have shown its usefulness in discriminating between metastatic or nonmetastatic lymph nodes during the EBUS procedure and, hence, the possibility of reducing unnecessary biopsies during mediastinal staging using EBUS-TBNA.

The vascular structure of a normal lymph node is distorted by tumor infiltration and neovascularization is observed in these metastatic lymph nodes in breast cancer and laryngeal cancer.[7,8] It is possible to observe these vascular changes by endoscopic or endobronchial ultrasound,[6,9,10] and these Doppler mode ultrasound findings may be related to tumor progression and patient survival in metastatic melanoma.[11] The neovascularization of tumors is known to correlate with several angiogenesis-related molecules, such as vascular endothelial growth factors (VEGFs).[12] Gene expression of *VEGF* is regulated by hypoxia inducible factor (HIF) and is affected by the hypoxic microenvironment of the tumor.[13] It is has been previously reported that high blood flow imaged by color power Doppler flow is associated with elevated VEGF protein level and increased risk of lymph node metastasis and poorer prognosis in patients with breast cancer.[14,15]

The expression of angiogenesis-related biomarkers reflects particular microenvironmental aspects of tumor tissue such as tissue hypoxia. Indeed, tissue hypoxia is a predictive factor for tumor response to radiotherapy.[16] In addition, mRNA expression of *VEGF* is known to be a prognostic

marker of NSCLC.[17] If we could demonstrate a correlation between the expression of angiogenesis-related molecules and Doppler mode ultrasound image findings, we could predict the angiogenesis-related molecular biomarker levels of lung cancer cells within metastatic lymph node. This would aid selection of treatment and help predict prognosis. The aim of this study was to assess the correlation between endobronchial ultrasound Doppler mode image patterns of mediastinal and/or hilar lymph nodes and the expression of angiogenesis-related molecules including *HIF-1α*, *VEGF-A*, and *VEGF-C*.

PATIENTS AND METHODS

Study Subjects

Patients with diagnosed lung cancer who underwent EBUS-TBNA using universal endoscopic ultrasound scanner (EU-ME1; Olympus, Tokyo, Japan) were retrospectively reviewed (from April 2009 to October 2009). The clinical lymph node samples obtained by EBUS-TBNA were archived with patients' agreement and used for analysis. Patients who had any prior treatment were excluded from this study. The definition of each lymph node location is as stated by the 7th edition of the Tumor Node Metastasis classification for lung cancer.[18] This research was approved by the ethics committee of Chiba Cancer Center (No. 20–21, No. 21–10, No. 21–52). Written consent was obtained from all patients. All samples were coded and managed independently.

Lymph Node Observation Using EBUS

EBUS procedures were performed on an outpatient basis in patients under conscious sedation (midazolam) with local anesthesia. The convex probe endobronchial ultrasound (BF-UC260FW; Olympus) equipped with a linear probe on its tip was used to perform EBUS-TBNA. The ultrasound image was processed in the universal endoscopic ultrasound scanner (EU-ME1) and a fixed frequency of 10-MHz observation mode used. Before Doppler mode observation, conventional B-mode observation was performed, and measurements made of the long and short axis of the lymph node. The Doppler mode image was captured as JPEG images while viewing the maximum diameter of the lymph node. In addition, the Doppler mode image was recorded in digital video format videotape and the vascular findings reviewed by three different individuals (TN, TA, and KY) blinded to the results of EBUS-TBNA. The final characteristics of the vascular findings for each lymph node were based on an agreement of at least two reviewers.[6]

EBUS Doppler Mode Image Characteristics of Lymph Nodes

EBUS procedures and Doppler mode image interpretations were performed in the same fashion as previously described.[6] The characters of the vascular structures within the lymph nodes were graded based on EBUS Power Doppler mode images classification system.[6] This classification system showed high intraobserver and interobserver agreement, which was considered to be almost perfect agreement (the Cohen's kappa value to assess the intraobserver variability was 0.830–0.853 and the Fleiss's kappa value of 3 interobserver variability was 0.83).[6] In this study, grade 0 and I were categorized as normal flow, grade II was categorized as low blood flow (LBF), and grade III was categorized as high blood flow (HBF) (Fig. 1).

Quantification of Vascular Index

For the quantitative analysis of vascular area within lymph node, we defined the vascular index ratio (VIR) (vascular percentage area) as vascular area (color pixel area) per lymph node area (gray pixel area) on EBUS Doppler mode image. The VIR was determined with ImageJ 1.45[19] (National Institutes of Health, Bethesda, MD) using the following image-processing steps (Fig. 2): (1) a binary image was created from the raw image, which is used for the determination of Doppler mode image classification; (2) a lymph node area was manually clipped as region of interest (ROI); (3) the vascular area that was visualized as color pixel area was determined with a certain threshold level (the same level for all sections); (4) ImageJ *measure* function was used to determine both, the area of ROI area (gray pixel) and vascular area (color pixel); (5) the percentage of vascular area on the ROI was calculated.

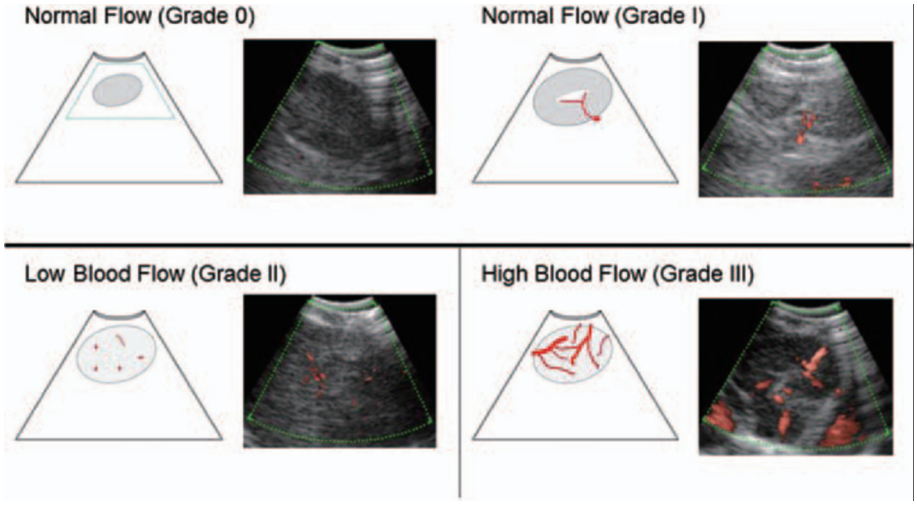

FIGURE 1. Endobronchial ultrasound-guided power Doppler mode images classification system. Grade 0: no blood flow or small amounts of flow, grade I: a few main vessels running toward the center of the lymph node from the hilum, grade II: a few punctiforms or rod-shapes of flow signal, a few small vessels found as a long strip of a curve, grade III: rich flow, more than four vessels found with different diameters and twist or helical-flow signal. Grade 0 and I were categorized as normal blood flow, grade II was categorized as low blood flow,, and grade III was categorized as high blood flow.

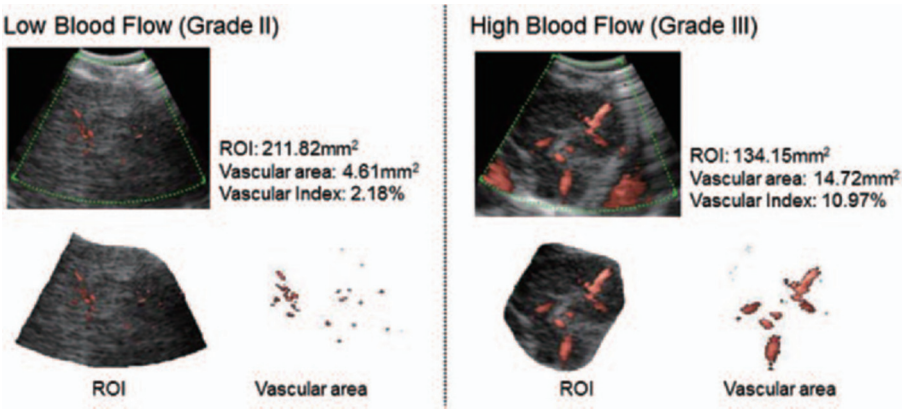

FIGURE 2. Quantification of vascular index using ImageJ. For the quantitative analysis of vascular area within lymph node, we defined the vascular index ratio (vascular percentage area) as vascular area (color pixel area) per region of interest (lymph node area) on endobronchial ultrasound-guided Doppler mode image. ROI, region of interest.

TABLE 1. The Sequences of Primers

B2M	5′ to 3′
Forward	GAGGCTATCCAGCGTACTCC
Reverse	CAATGTCGGATGGATGAAAC
HIF1-α	5′ to 3′
Forward	GGCAGCAACGACACAGAAAC
Reverse	TGATTGAGTGCAGGGTCAGC
VEGF-A	5′ to 3′
Forward	CTACTGCCATCCAATCGAGAC
Reverse	AATCTGCATGGTGATGTTGG
VEGF-C	5′ to 3′
Forward	GCCAACCTCAACTCAAGGAC
Reverse	CCCACATCTGTAGACGGACA

EBUS-TBNA Procedure, Sample Storage, Isolation of RNA and Protein

EBUS-TBNA was performed to the same targeted lymph node as observed by Doppler mode. The procedures of EBUS-TBNA were performed in the same fashion as previously described.[20,21] Rapid onsite cytology was not performed; however, an independent pathologist reviewed all cases and pathologically confirmed the presence or absence of NSCLC cells in each specimen. The procedures of EBUS-TBNA, sample storage, and isolation of RNA and protein were performed in the same fashion as previously described.[22,23]

Quantitative Real-Time Reverse Transcription Polymerase Chain Reaction

QuantiTect Reverse Transcription Kit (QIAGEN Inc., Valencia, CA) was used for reverse transcription. Quantitative real-time RT-PCR was performed in a LightCycler 480 (Roche Applied Science, Indianapolis, IN) using a LightCycler 480 SYBR Green I Master (Roche) in a total volume of 20 mL. The samples were analyzed in duplicates. Human β2 microglobulin was selected as a housekeeping gene, which was used for internal control of gene expression analysis. *HIF-1α*, *VEGF-A,* and *VEGF-C* were selected as an angiogenesis-related genes in this study (Table 1).

Measurement of Protein Expression

Targeted protein levels in the sample were determined using enzyme-linked immunoassay kit (Surveyor IC, Quantikine Immunoassay; R&D systems, Minneapolis, MN). These protein levels were normalized using total protein content measured by the Bio-Rad Protein Assay (Bio-Rad Laboratories, Hercules, CA). Finally, the expression ratio of targeted protein (target protein level [pg/mL]/protein concentration [μg/μL]) was calculated and analyzed.

Data Analysis

Statistical comparisons were made using the Mann–Whitney *U* test. General data analysis was conducted using JMP 8.0 (SAS Institute Inc., Cary, NC). All *p* values were based on a two-sided hypothesis, with *p* values less than 0.05 considered to have statistical significance.

RESULTS

Patients and Analyzed Samples

Thirty-eight archived clinical EBUS-TBNA samples were analyzed. There were 27 metastatic lymph nodes (17 adenocarcinoma, 6 squamous cell carcinoma, 4 poorly differentiated NSCLC) and 11 nonmetastatic lymph nodes. The characteristics of the lymph nodes analyzed in this study are summarized in Table 2. All nonmetastatic lymph nodes were graded as normal flow (grade 0 or I). Within the 27 positive lymph nodes, eight were categorized as LBF (grade II) and 19 were categorized as HBF (grade III). The size of sampled lymph nodes ranged from 6.9 mm to 33.4 mm on EBUS imaging and was significantly larger in metastatic lymph nodes ($p = 0.0252$). Station #4R and #7 were most frequently sampled in metastatic lymph nodes, and #11 was most frequently sampled in nonmetastatic lymph nodes. Twenty-five of 27 metastatic lymph nodes (92.6%) showed standardized uptake value more than 2.5, which was considered as positive for malignancy by ^{18}F-fluorodeoxy glucose-positron emission tomography.

VIR Analysis in Metastatic Lymph Node

The mean pixel values of the lymph node area, which were visualized as gray pixel, were 216.70 mm^2 (range, 148.74–299.59) in the LBF group and 187.06 mm^2 (range,

76.41–342.19) in the HBF group. The mean pixel values of vascular area, which were visualized as color pixel, were 5.34 mm^2 (range, 2.26–10.50) in the LBF group and 13.44 mm^2 (range, 3.83–33.6) in the HBF group. VIR was significantly higher in the HBF group (7.26% [range, 2.40%–13.75%]) than in the LBF group (2.54% [range, 1.49%–5.52%]) ($p = 0.0003$).

RNA and Protein Extraction

Total RNA was successfully isolated in all 38 samples. The median amount of isolated RNA was 6.85 μg from the nonmetastatic lymph node (range, 2.27–16.42) and 15.17 μg from the metastatic lymph node (range, 2.00–61.22). The mean ratio of absorptions at 260 versus 280 nm for the purity of RNA was 1.83.

Protein was also successfully isolated in all 38 samples. The median amount of isolated protein was 4.25 mg (range, 2.18–6.65) from the nonmetastatic lymph node and 3.44 mg (range, 0.17–12.46) from the metastatic lymph node.

TABLE 2. Characteristics of Analyzed Lymph Nodes

	Metastatic LN	Nonmetastatic LN	*p*
n	27	11	
Histology type of primary tumor			
Adenocarcinoma	17	6	
Squamous cell carcinoma	6	3	
Poorly differentiated NSCLC	4	2	
Sampled lymph node station			
2R	3	0	
4R	10	2	
4L	2	1	
7	9	3	
11	3	5	
Mean LN size of CT (short axis, range)	21.4 (10–37)	15.3 (10–39)	*0.1315*
Mean LN size of EBUS (short axis, range)	18.1 (8.3–33.4)	13.4 (6.9–25.4)	*0.0252*
Doppler grade			
NBF (Grade 0–I)	0	11	
LBF (Grade II)	8	0	
HBF (Grade III)	19	0	

LN, lymph node; NSCLC, non–small-cell lung cancer; NBF, normal blood flow; LBF, low blood flow; HBF, high blood flow.

mRNA Expression Levels of Angiogenesis-Related Genes

Gene expression levels of *HIF1-α*, *VEGF-A*, and *VEGF-C* were quantifiable in all samples. The mRNA expression levels relative to human β2 microglobulin are shown in Table 3.

HIF1-α ($p < 0.0001$) and *VEGF-A* ($p < 0.0001$) mRNA were expressed significantly higher in the metastatic lymph node versus the nonmetastatic lymph node. There was no significant difference for VEGF-C ($p = 0.6756$) between metastatic and nonmetastatic lymph nodes (Fig. 3).

Within metastatic lymph nodes, there were significant differences for *HIF1-α* and *VEGF-C* mRNA expressions. *HIF1-α* had significantly higher expression in the LBF group ($p = 0.01$), and *VEGF-C* had significantly higher expression in the HBF group ($p = 0.0315$), vice versa. Interestingly, there was no significant difference for *VEGF-A* expression between the LBF and HBF groups ($p = 0.5069$) (Fig. 4).

Enzyme-Linked Immunoassay

Protein expression levels of HIF1-α, VEGF-A ($VEGF\text{-}A_{165}$), and VEGF-C were quantified. Three out of 38 samples for VEGF-A ($VEGF\text{-}A_{165}$) and one out of 38 samples for VEGF-C could not be measured because of low protein concentration. The protein expression ratios were shown in Table 4.

There was no significant difference in HIF1-α ($p = 0.9743$), VEGF-A ($VEGF\text{-}A_{165}$) ($p = 0.1386$), and VEGF-C protein expression ($p = 0.6522$) between metastatic and nonmetastatic lymph nodes. Within metastatic lymph nodes, there were also no significant differences for HIF1-α ($p = 0.3259$), VEGF-A ($VEGF\text{-}A_{165}$) ($p = 0.2761$), and VEGF-C ($p = 0.1757$) protein expression between the LBF and HBF groups.

DISCUSSION

We have recently reported that the Doppler mode vascular image finding classification system of lymph nodes during EBUS can be used to distinguish between metastatic and nonmetastatic lymph nodes in patients with lung cancer.[6] There were two subtypes within the group of metastatic lymph nodes, which again, could be classified by blood-flow pattern: Grade II—LBF and Grade III—HBF.[6] In this study, we examined the expression of angiogenesis-related molecules within lymph nodes and revealed a correlation between Doppler mode ultrasound findings and molecular

TABLE 3. mRNA Expression Levels Relative to *B2M*

	Median mRNA Expression Levels Relative to *B2M*					
	HIF1-α		*VEGF-A*		*VEGF-C*	
Nonmetastatic LN	0.68 (0.26–0.89)		0.03 (0.01–0.04)		0.08 (0.01–0.19)	
Metastatic LN	1.91 (0.76–6.97)	$p < 0.0001$	1.01 (0.03–19.4)	$p < 0.0001$	0.07 (0.002–2.8)	$p = 0.6756$
LBF group	2.39 (1.15–5.49)		1.15 (0.57-7.67)		0.03 (0.01–0.14)	
HBF group	1.50 (0.76–6.97)	$p = 0.01$	0.91 (0.03–19.4)	$p = 0.5069$	0.10 (0.002–2.8)	$p = 0.0315$

LN, lymph node; LBF, low blood flow; HBF, high blood flow.

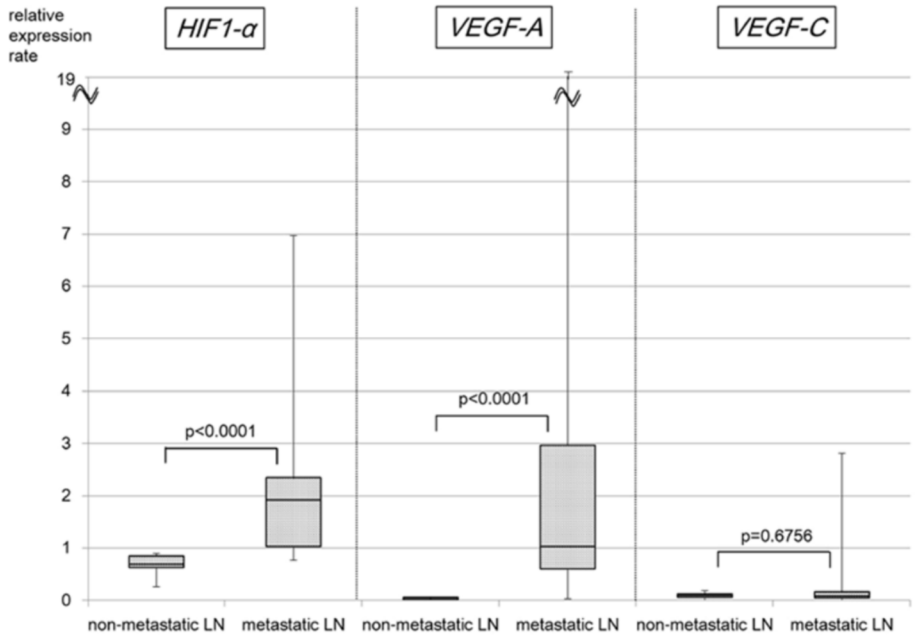

FIGURE 3. mRNA expression levels between nonmetastatic lymph nodes and metastatic lymph nodes. *HIF1-α* ($p < 0.0001$) and *VEGF-A* ($p < 0.0001$) mRNA were significantly more highly expressed in the metastatic lymph node than in the nonmetastatic lymph node. There was no significant difference for *VEGF-C* ($p = 0.6756$) between metastatic and nonmetastatic lymph nodes. LN, lymph node.

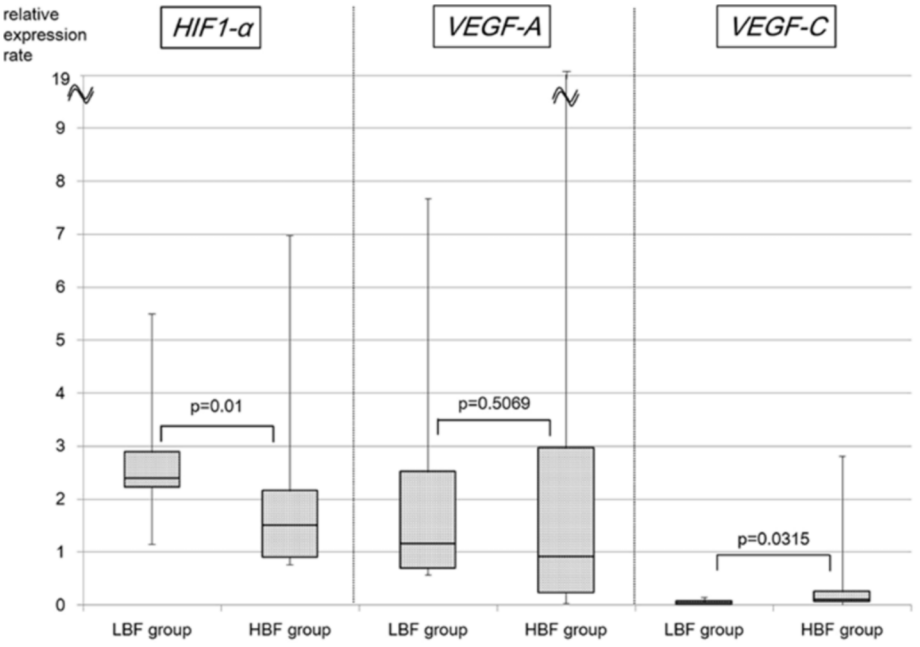

FIGURE 4. mRNA expression levels between the LBF group and the HBF group. Within metastatic lymph nodes, there were significant differences in *HIF1-α* and *VEGF-C* mRNA expressions. *HIF1-α* had significantly higher expression in the LBF group ($p = 0.01$), and *VEGF-C* had significant higher expression in the HBF group ($p = 0.0315$) and vice versa. However, there was no significant difference for *VEGF-A* between the LBF and HBF groups ($p = 0.5069$). LBF, low blood flow; HBF, high blood flow.

TABLE 4. Protein Expression Ratios

	Median Protein Expression Ratio (target protein/total protein)					
	HIF1-α		**VEGF-A ($VEGF_{165}$)**		**VEGF-C**	
Nonmetastatic LN	20.71 (11.37–97.56)		32.84 (3.39–92.25)		810.77 (147.40–3114.93)	
Metastatic LN	20.92 (3.78–275.71)	$p = 0.9743$	14.27 (0–290.65)	$p = 0.1386$	711.75 (0–5526.22)	$p = 0.6522$
LBF group	45.85 (3.78–275.71)		7.42 (0–290.65)		267.65 (0–5526.22)	
HBF group	20.40 (11.68–140.82)	$p = 0.3259$	14.80 (0–205.32)	$p = 0.2761$	732.62 (134.78–4353.74)	$p = 0.1757$

VEGF, vascular endothelial growth factor; HIF1, hypoxia inducible factor; LN, lymph node; LBF, low blood flow; HBF, high blood flow.

markers. Metastatic lymph nodes had significantly higher expression of both HIF1-α and VEGF-A than nonmetastatic nodes did. Furthermore, *HIF1-α* mRNA had significantly higher expression in the LBF group, and *VEGF-C* mRNA had significantly higher expression in the HBF group. This result may suggest the higher mRNA expression of *HIF1-α* in the LBF group may be induced by tissue hypoxia caused by LBF, and the higher mRNA expression of *VEGF-C* in the HBF group may result from the HBF within metastatic lymph nodes. Another explanation could be HIF1-α is first generated in a hypoxic state of metastatic lymph nodes, which causes high expression of VEGF-A, then subsequently increases the expression of VEGF-C; this is then seen in HBF lymph nodes.

The molecular markers analyzed in this study (HIF1-α, VEGF-A, and VEGF-C) are recognized as correlating with tissue oxygenation (hypoxia) and tumor angiogenesis. Hypoxia has been shown to be a major inducer of VEGF gene transcription.[24] VEGF-A is known as the major mediator of tumor angiogenesis. VEGF-A is highly expressed in most types of human cancer cells.[24] VEGF-C plays a major role in tumor lymphangiogenesis and expresses with its receptor (R), VEGFR-3, in lymphatic endothelial cells.[25] These biomarkers have been identified as predictive factors for the response to radiotherapy and chemotherapy.[16,26] In addition, the mRNA expression of *VEGF* is established as a prognostic marker of NSCLC.[17] Improvements in the tissue hypoxic microenvironment by drugs may lead to change in the expression of these molecules and enhance treatment efficacy.[27–29] VEGF-C is known to be related to lymphangiogenesis, lymph node metastasis, and poor prognosis in patients with lung cancer.[30–33] In addition, VEGF-C is known to be an important target molecule in the regulation of lymph node and distant metastasis of cancer.[34]

Recently, the VEGF pathway has been targeted in patients with advanced NSCLC, by using therapy using bevacizumab with significant improvement of progression-free survival and overall survival.[35] Bevacizumab is a humanized monoclonal antibody that inhibits VEGF-A.[36] In addition to this anti-VEGF antibody, VEGF receptor tyrosine kinase inhibitors, such as pazopanib, have been developed. Pazopanib is a multitargeted tyrosine kinase receptor inhibitor of VEGFR-1, VEGFR-2, VEGFR-3, platelet-derived growth factor receptor-a/β, and c-kit (receptors). This drug has demonstrated an 86% reduction in tumor volume when administered as a short-term preoperative treatment in patients with early-stage NSCLC.[37] As shown in this study, VEGF-C is also highly expressed in metastatic lymph nodes; therefore, multitargeted VEGFR tyrosine kinase inhibition may be more effective for the treatment of locally advanced NSCLC.

One potential limitation of our study is protein analysis using EBUS-TBNA samples. As previously described, samples obtained by EBUS-TBNA consisted mainly of tumor cells, blood constituent, and a small amount of lymph node tissue.[38] Compared with the number of tumor cells, there was relatively little representation of normal or reactive tissue within the samples. Therefore, EBUS-TBNA samples can easily be used for genetic analysis. However, one potential limiting factor to using enzyme-linked immunosorbent assay analysis for EBUS samples is the presence of blood. Blood contamination causes hemodilution, affecting the results of protein analysis and this effect is varied by the degree of blood contamination. The mean value of HIF1-α, VEGF-A, and VEGF-C protein is higher in the LBF group; however, there was no significant difference even between metastatic and nonmetastatic lymph nodes. Another limitation of this study is also related to quantity and quality of samples obtained by this needle biopsy procedure. The *core* can be used for histological evaluation; however, it is basically cytological material.[39] It is hard to obtain structured tissue that can be used for microvascular and lymphatics density evaluation by immunohistochemistry. It is known that several kinds of cells can produce and release VEGFs, including tumor cells, macrophages and monocytes, and signaling to VEGFRs on endothelial cells that regulate neovascularization. It is also difficult to identify VEGFs producing cells and endothelial cells within the EBUS-TBNA samples. Further investigation will be needed to confirm this result and may need to evaluate surgically resected specimens.

In conclusion, this study was based on a limited number of samples; we have, however, demonstrated a significant association between Doppler mode findings and angiogenesis-related molecules. The Doppler mode image findings of lymph nodes may provide us with additional information regarding the tumor microenvironment within metastatic lymph nodes. To evaluate this relationship fully, a large number of case series needs to be assessed so that these findings can be validated and applied clinically.

ACKNOWLEDGMENTS

The authors thank Ms. Guan Zehong for technical assistance. The authors also thank Mr. Tetsushi Hirata and Dr. Makiko Itami (Chiba Cancer Center) for pathological diagnosis.

REFERENCES

1. Gu P, Zhao YZ, Jiang LY, Zhang W, Xin Y, Han BH. Endobronchial ultrasound-guided transbronchial needle aspiration for staging of lung cancer: a systematic review and meta-analysis. *Eur J Cancer* 2009;45:1389–1396.
2. Adams K, Shah PL, Edmonds L, Lim E. Test performance of endobronchial ultrasound and transbronchial needle aspiration biopsy for mediastinal staging in patients with lung cancer: systematic review and meta-analysis. *Thorax* 2009;64:757–762.
3. Yasufuku K, Pierre A, Darling G, et al. A prospective controlled trial of endobronchial ultrasound-guided transbronchial needle aspiration compared with mediastinoscopy for mediastinal lymph node staging of lung cancer. *J Thorac Cardiovasc Surg* 2011;142:1393–400.e1.
4. Memoli JS, El-Bayoumi E, Pastis NJ, et al. Using endobronchial ultrasound features to predict lymph node metastasis in patients with lung cancer. *Chest* 2011;140:1550–1556.
5. Fujiwara T, Yasufuku K, Nakajima T, et al. The utility of sonographic features during endobronchial ultrasound-guided transbronchial needle aspiration for lymph node staging in patients with lung cancer: a standard endobronchial ultrasound image classification system. *Chest* 2010;138:641–647.
6. Nakajima T, Anayama T, Shingyoji M, Kimura H, Yoshino I, Yasufuku K. Vascular image patterns of lymph nodes for the prediction of metastatic disease during EBUS-TBNA for mediastinal staging of lung cancer. *J Thorac Oncol* 2012;7:1009–1014.
7. Adler DD, Carson PL, Rubin JM, Quinn-Reid D. Doppler ultrasound color flow imaging in the study of breast cancer: preliminary findings. *Ultrasound Med Biol* 1990;16:553–559.
8. Zhou J, Zhu SY, Liu RC, Luo F, Shu DX. Vascularity index of laryngeal cancer derived from 3-D ultrasound: a predicting factor for the in vivo assessment of cervical lymph node status. *Ultrasound Med Biol* 2009;35:1596–1600.

9. Sawhney MS, Debold SM, Kratzke RA, Lederle FA, Nelson DB, Kelly RF. Central intranodal blood vessel: a new EUS sign described in mediastinal lymph nodes. *Gastrointest Endosc* 2007;65:602–608.
10. Nakajima T, Shingyouji M, Nishimura H, et al. New endobronchial ultrasound imaging for differentiating metastatic site within a mediastinal lymph node. *J Thorac Oncol* 2009;4:1289–1290.
11. Voit C, Van Akkooi AC, Schäfer-Hesterberg G, et al. Ultrasound morphology criteria predict metastatic disease of the sentinel nodes in patients with melanoma. *J Clin Oncol* 2010;28:847–852.
12. Fontanini G, Vignati S, Boldrini L, et al. Vascular endothelial growth factor is associated with neovascularization and influences progression of non-small cell lung carcinoma. *Clin Cancer Res* 1997;3:861–865.
13. Koshikawa N, Iyozumi A, Gassmann M, Takenaga K. Constitutive upregulation of hypoxia-inducible factor-1alpha mRNA occurring in highly metastatic lung carcinoma cells leads to vascular endothelial growth factor overexpression upon hypoxic exposure. *Oncogene* 2003;22:6717–6724.
14. Wang Y, Dan HJ, Fan JH, Wen SB. Evaluation of the correlation between colour power Doppler flow imaging and vascular endothelial growth factor in breast cancer. *J Int Med Res* 2010;38:1077–1083.
15. Chen CN, Lin JJ, Lee H, et al. Association between color doppler vascularity index, angiogenesis-related molecules, and clinical outcomes in gastric cancer. *J Surg Oncol* 2009;99:402–408.
16. Pore N, Gupta AK, Cerniglia GJ, et al. Nelfinavir down-regulates hypoxia-inducible factor 1alpha and VEGF expression and increases tumor oxygenation: implications for radiotherapy. *Cancer Res* 2006;66:9252–9259.
17. Yuan A, Yu CJ, Kuo SH, et al. Vascular endothelial growth factor 189 mRNA isoform expression specifically correlates with tumor angiogenesis, patient survival, and postoperative relapse in non-small-cell lung cancer. *J Clin Oncol* 2001;19:432–441.
18. Rusch VW, Asamura H, Watanabe H, Giroux DJ, Rami-Porta R, Goldstraw P; Members of IASLC Staging Committee. The IASLC lung cancer staging project: a proposal for a new international lymph node map in the forthcoming seventh edition of the TNM classification for lung cancer. *J Thorac Oncol* 2009;4:568–577.
19. Rasband, WS. Image J. Bethesda, MD: U. S. National Institutes of Health, http://imagej.nih.gov/ij/, 1997–2011. Accessed March 1, 2011.
20. Yasufuku K, Nakajima T, Motoori K, et al. Comparison of endobronchial ultrasound, positron emission tomography, and CT for lymph node staging of lung cancer. *Chest* 2006;130:710–718.
21. Nakajima T, Yasufuku K, Iyoda A, et al. The evaluation of lymph node metastasis by endobronchial ultrasound-guided transbronchial needle aspiration: crucial for selection of surgical candidates with metastatic lung tumors. *J Thorac Cardiovasc Surg* 2007;134:1485–1490.
22. Nakajima T, Yasufuku K. How I do it–optimal methodology for multidirectional analysis of endobronchial ultrasound-guided transbronchial needle aspiration samples. *J Thorac Oncol* 2011;6:203–206.
23. Nakajima T, Anayama T, Koike T, et al. Simultaneous isolation of total RNA, DNA, and protein using samples obtained by EBUS-TBNA. *J Bronchol Intervent Pulmonol* 2011;18:301–305.
24. Kerbel RS. Tumor angiogenesis. *N Engl J Med* 2008;358:2039–2049.
25. Stacker SA, Achen MG, Jussila L, Baldwin ME, Alitalo K. Lymphangiogenesis and cancer metastasis. *Nat Rev Cancer* 2002;2:573–583.
26. Ogawa K, Chiba I, Morioka T, et al. Clinical significance of HIF-1alpha expression in patients with esophageal cancer treated with concurrent chemoradiotherapy. *Anticancer Res* 2011;31:2351–2359.
27. Yasuda H, Nakayama K, Watanabe M, et al. Nitroglycerin treatment may enhance chemosensitivity to docetaxel and carboplatin in patients with lung adenocarcinoma. *Clin Cancer Res* 2006;12:6748–6757.
28. Yasuda H, Yamaya M, Nakayama K, et al. Randomized phase II trial comparing nitroglycerin plus vinorelbine and cisplatin with vinorelbine and cisplatin alone in previously untreated stage IIIB/IV non-small-cell lung cancer. *J Clin Oncol* 2006;24:688–694.
29. Shinohara ET, Maity A. Increasing sensitivity to radiotherapy and chemotherapy by using novel biological agents that alter the tumor microenvironment. *Curr Mol Med* 2009;9:1034–1045.
30. Anagnostou VK, Tiniakos DG, Fotinou M, Achimastos A, Syrigos KN. Multiplexed analysis of angiogenesis and lymphangiogenesis factors predicts outcome for non-small cell lung cancer patients. *Virchows Arch* 2011;458:331–340.
31. Saintigny P, Kambouchner M, Ly M, et al. Vascular endothelial growth factor-C and its receptor VEGFR-3 in non-small-cell lung cancer: concurrent expression in cancer cells from primary tumour and metastatic lymph node. *Lung Cancer* 2007;58:205–213.
32. Arinaga M, Noguchi T, Takeno S, Chujo M, Miura T, Uchida Y. Clinical significance of vascular endothelial growth factor C and vascular endothelial growth factor receptor 3 in patients with nonsmall cell lung carcinoma. *Cancer* 2003;97:457–464.
33. Kajita T, Ohta Y, Kimura K, et al. The expression of vascular endothelial growth factor C and its receptors in non-small cell lung cancer. *Br J Cancer* 2001;85:255–260.
34. Hirakawa S, Brown LF, Kodama S, Paavonen K, Alitalo K, Detmar M. VEGF-C-induced lymphangiogenesis in sentinel lymph nodes promotes tumor metastasis to distant sites. *Blood* 2007;109:1010–1017.
35. Sandler A, Gray R, Perry MC, et al. Paclitaxel-carboplatin alone or with bevacizumab for non-small-cell lung cancer. *N Engl J Med* 2006;355:2542–2550.
36. Los M, Roodhart JM, Voest EE. Target practice: lessons from phase III trials with bevacizumab and vatalanib in the treatment of advanced colorectal cancer. *Oncologist* 2007;12:443–450.
37. Altorki N, Lane ME, Bauer T, et al. Phase II proof-of-concept study of pazopanib monotherapy in treatment-naive patients with stage I/II resectable non-small-cell lung cancer. *J Clin Oncol* 2010;28:3131–3137.
38. Nakajima T, Yasufuku K, Suzuki M, et al. Assessment of epidermal growth factor receptor mutation by endobronchial ultrasound-guided transbronchial needle aspiration. *Chest* 2007;132:597–602.
39. Nakajima T, Yasufuku K, Takahashi R, et al. Comparison of 21-gauge and 22-gauge aspiration needle during endobronchial ultrasound-guided transbronchial needle aspiration. *Respirology* 2011;16:90–94.

